American Mineralogist, Volume 83, pages 1551–1563, 1998

Experimental observations of the effects of bacteria on aluminosilicate weathering

W.W. BARKER,[1,*] **S.A. WELCH,**[2] **S. CHU,**[3] AND **J.F. BANFIELD**[1,2]

[1]Department of Geology and Geophysics, University of Wisconsin-Madison, Madison, Wisconsin 53706, U.S.A.
[2]Mineralogical Institute, University of Tokyo, Hongo, Bunkyo-ku, Tokyo 135, Japan
[3]Division of Gastroenterology, Departments of Medicine and Physiology, Johns Hopkins University School of Medicine, Baltimore, Maryland 21205, U.S.A.

ABSTRACT

Mineral dissolution experiments using batch cultures of soil and groundwater bacteria were monitored with solution chemistry and various microscopic techniques to determine the effects of these organisms on weathering reactions. Several strains of bacteria produced organic and inorganic acids and extracellular polymers in culture, increasing the release of cations from biotite (Si, Fe, Al) and plagioclase feldspar (Si, Al) by up to two orders of magnitude compared to abiotic controls. Microbial colonies on mineral grains were examined by cryo-scanning electron microscopy (cryo-SEM), confocal scanning laser microscopy (CSLM), and epifluorescence microscopy. Bacteria colonized all mineral surfaces, often preferentially along cleavage steps and edges of mineral grains. Low-voltage high-resolution cryo-SEM of high-pressure cryofixed and partially freeze-dried colonized minerals showed many bacteria attached by extracellular polymers of unknown composition. These biofilms covered much larger areas of the mineral surfaces than bacterial cells alone. Mineral surfaces where bacteria and extracellular polymers occurred appeared more extensively etched than surrounding uncolonized surfaces. CSLM was used to observe microbial colonization of biotite and to measure pH in microenvironments surrounding living microcolonies using a ratiometric pH-sensitive fluorescent dye set. A strain of bacteria (B0693 from the U.S. Department of Energy Subsurface Microbial Culture Collection) formed large attached microcolonies, both on the outer (001) surface and within interlayer spaces as narrow as 1 μm. Solution pH decreased from near neutral at the mineral surface to 3–4 around microcolonies living within confined spaces of interior colonized cleavage planes. However, no evidence of pH microgradients surrounding exterior microcolonies was noted.

INTRODUCTION

Mineral weathering is arguably one of the most important geochemical phenomena occurring at and near the Earth's surface. This process results in the formation of soils and maintenance of soil productivity; the evolution of ground, surface, and sea water composition; the denudation of continents; and regulation of atmospheric composition and global climate. Weathering is inextricably bound to biological processes, for organisms inhabit a wide range of niches in surface and subsurface environments and influence various mineral transformation reactions (Banfield and Nealson 1997; Huang and Schnitzer 1986).

Field observations and laboratory experiments demonstrate that microbes can accelerate aluminosilicate mineral weathering reactions, especially when in direct contact with mineral surfaces (see Barker et al. 1997 for a review), by producing organic and inorganic acids, producing metal-complexing ligands, changing redox conditions, or mediating formation of secondary mineral phases.

The physical size of pores exerts a primary control over distribution of microorganisms within rocks, soils, and sediments. Recent studies of the intact organic mineral interface of weathering silicates (Barker and Banfield 1998) in lithobiontic microbial communities have demonstrated a zonation defined by access of microorganisms to mineral surfaces. In the case of outcrop surfaces colonized by lichens, Barker and Banfield (1996, 1998) demonstrated that mineral weathering is accelerated beneath lichen thalli along fluid conduits such as cleavages and grain boundaries of insufficient size to permit microbial colonization (the indirect biochemilithic zone), presumably by soluble organic acids. Mineral reactions and textures approximate those seen in strictly physiochemical weathering, differing primarily in the extent to which they are developed. Where sufficient space exists to allow microbial access (the direct biochemilithic zone), all mineral surfaces, both primary and secondary phases, are coated in thick layers of microbial exopolymers, primarily acidic mucopolysaccharides. Assemblages of secondary miner-

---

* E-mail: barker@geology.wisc.edu

0003–004X/98/1112–1551$05.00

als, which differ in texture and chemistry from those formed in physiochemical weathering, develop within the enclosing polymer layers as the primary mineral phase dissolves.

Indirect biochemilithic mechanisms

Aluminosilicate dissolution rates are a function of pH; in general, rates are lowest near neutral pH and then increase with either increasing or decreasing acidity (Blum and Lasaga 1988). Low molecular weight organic ligands accelerate mineral weathering reactions by complexing with ions on the mineral surface or in solution. Organic acids are particularly effective for increasing the solubility and release rate of elements like Al and Fe (Welch and Ullman 1993; Stone 1997; Antweiler and Drever 1983). Under anoxic conditions, microbial production of organic acids by fermentation, or reductive dissolution of Fe-Mn mineral phases can greatly accelerate weathering rates of aluminosilicate minerals (Welch 1996; Ehrlich 1996; Bennett et al. 1996).

Direct biochemilithic mechanisms

Microbial cell surfaces and extracellular polymers serve as templates for the formation of secondary mineral phases (Barker and Banfield 1996, 1998; Fortin et al. 1997). Microorganisms produce various extracellular polymers (primarily proteins and polysaccharides) that serve as attachment structures to anchor cells to the substratum. Microbes also synthesize exopolymers to form thick gel layers or biofilms, one advantage of which is thought to be the creation of controllable microenvironments around microbial cells (Christensen and Characklis 1990). Polysaccharides are known to play an antidesiccant role in microorganisms (Ophir and Gutnick 1994). An important effect of microbial attachment and biofilm formation on aluminosilicate weathering may simply be to increase the residence time of water, as compared to the residence time at the bare rock surface. Additionally, polysaccharide coatings on mineral grains serve to maintain diffusion pathways as water potential decreases in soils (Chenu and Roberson 1996). Recently, experiments with simple acid polysaccharides have shown that these compounds interact chemically with minerals, and can both increase and decease mineral dissolution rates, depending on pH (Welch et al., in preparation). Because intimate contact between hydrous polymers and the mineral surface can affect reaction rates, an understanding of the true three-dimensional structure of microbial polymer layers and the extent of polymeric mineral surface coverage is important. Knowledge of cell distribution within these films as well as among and within the interior of mineral grains, and the nature of chemical microenvironments that form and are maintained by living cells, is equally central to evaluating microbial involvement in mineral weathering.

To better understand the role of bacteria and their metabolites on aluminosilicate mineral weathering in nature, we conducted a series of experiments to determine the distribution of bacteria on feldspar and biotite surfaces and the abundance and distribution of their associated polymers. Because of the strong dependence of most mineral dissolution rates on pH, it is particularly important to quantify the pH variation in proximity to living cells. Consequently, we measured the pH of microenvironments adjacent to microbial colonies to evaluate microbial impact on mineral dissolution rates. In this paper we present results of experimental abiotic and biotic weathering studies, couple these results to an analysis of extracellular polymer structure and distribution, and provide new insights into how attached bacteria impact mineral weathering.

METHODS

Rationale

Microbial polysaccharides contain greater than 99% water (Sutherland 1972) and are extremely difficult to prepare for the high-vacuum environment of the electron microscope. Air drying, critical point drying for SEM, as well as standard chemical fixations and embedding techniques for TEM all introduce severe dehydration artifacts. Critical point drying, freeze drying, and freeze etch replication all circumvent surface tension forces associated with air-dried samples, although these techniques too can produce experimental artifacts. Critical point drying involves the replacement of water by alcohol that is in turn exchanged for liquid CO_2, although the harsh chemical treatment used in critical point drying can damage delicate organic structures. Recent biofilm studies using environmental SEMs have resulted in a better understanding of the overall dimensions of fully hydrated gels (Little et al. 1997), but resolution limitations of these instruments preclude gathering information concerning the three-dimensional ultrastructure of polysaccharide surface coatings.

Cryofixation and appropriate cryomicroscopic techniques appear to offer the best possibility for studying these gels in their true hydrated state. The goal of all cryofixation techniques is to freeze the water component rapidly and prevent sample damage from ice crystal nucleation and growth [see Echlin (1992) and Steinbrecht and Zierold (1987) for thorough discussions of low-temperature microscopy techniques], resulting in an amorphous solid known as vitreous ice. Poorly frozen samples display various artifacts attributable to ice crystallization. In particular, one type of artifact in cryofixation of hydrated polymers is solute migration, formed by exclusion of all components except water from ice crystals as they nucleate and grow. Solute migration artifacts are well documented, however, and easy to recognize. In the case of polysaccharides, all fine structure is destroyed and the polymers appear as large strands, often described as cobwebbed. Ultrarapid cryofixation is achieved by various rapid freezing techniques such as propane jet cryofixation, plunge freezing, and slam freezing. Under optimal conditions, vitreous ice forms as a thin layer that approaches a thickness of 10 μm under optimal conditions. We chose another method, high-pressure cryofixation, because it offers the potential for achieving vitreous ice in much larger volumes, in some cases up to 1 mm^3. The ability to achieve vitreous ice conditions in samples of these dimensions enabled us to cryofix and examine individual mineral grains carrying well-developed biofilms. The sample (maintained at liquid nitrogen temperatures and under vacuum to expose a noncontaminated surface) is transferred to a cryo-coating unit. The sample temperature is increased to initiate ice sublimation, which exposes nonvolatile components, a process referred to as "etching." High-pressure cryofixation and cryo-SEM preserves the delicate three-dimensional structure of mineral organic interactions (Defarge et al. 1996). Spontaneous fracture is a characteristic of high-pressure frozen samples, in which large cracks form in the sample during cryofixation. One advantage of spontaneous fracturing prior to etching is that cross-sectional views through the biofilm polymer are available for study. A thin coating (2 nm) of platinum or chromium is applied to prevent charging and the sample is held at −95 °C with a cryostage and examined in a high-resolution, field-emission, low-voltage SEM.

Confocal scanning laser microscopy (CSLM) allows examination of a fluorescing sample in three dimensions by collecting a series of digitized optical sections that can be manipulated via computer (Pawley 1995). CSLM has been applied sparingly in geological research, primarily to examine porosity in sandstone (Fredrich et al. 1995), weathering (Rautureau et al. 1993), and fission track orientation in minerals (Petford and Miller 1992). In contrast, confocal microscopy has been applied widely in the biological sciences. The technique has been used to study film thickness, distribution of microorganisms (Lawrence et al. 1991), fluid flow (Stoodley et al. 1994), and diffusion coefficients within biofilms (Lawrence et al. 1994). But most importantly for geomicrobiological applications, CSLM can be used to examine fully hydrated samples and living microbial cells in vivo and to make quantitative measurements regarding ion concentrations and pH. Microelectrodes also have been used to study pH gradients within biofilms (Parasuraman 1995), but are not appropriate for measurements in micrometer-sized spaces commonly occupied by microbes within mineral grains.

Ratiometric pH-sensitive fluorescent probes have been used to measure intracellular and extracellular pH gradients in microenvironments. This technique has been applied to measure pH gradients in colonic crypts (Chu and Montrose 1995; Chu et al. 1995), plant cells (Roos 1992), and surrounding lactic-acid bacteria forming yogurt (Hassan et al. 1995a, 1995b). In this study, we used a ratiometric method (Chu et al. 1995) to measure pH changes around bacterial microcolonies attached to biotite.

Bacteria

Five strains of bacteria (B0428, C0564, B0577, B0665, B0693) were obtained from the U.S. Department of Energy Subsurface Microbial Culture Collection from David Balkwill, Florida State University, for these experiments. These strains, which are naturally occurring subsurface bacteria, were chosen for their ability to produce organic acids or extracellular polymers (Vandevivere et al. 1994; Welch and Vandevivere 1994). Strain B0428 was isolated from the PeeDee Formation, whereas all other strains were isolated from the Middendorf Formation at the Savannah River site, South Carolina. Strains B0665 and B0693 have been tentatively identified based on 16sRNA sequences (Welch and Barker, unpublished data). B0665 is a β-Proteobacteria, very closely related to *Burkholderia solanacearum,* whereas B06093 is a gram positive *Arthrobacter* species. The bacteria were grown in a sterilized 1% peptone-yeast-glucose media for 2–3 d and then harvested for dissolution experiments by centrifugation at 5000 rpm. Cell pellets were then resuspended and rinsed several times in sterile deionized water to remove culture media before the dissolution experiments.

Mineral preparation

Bulk samples of bytownite feldspar and biotite were purchased from Wards Scientific. Samples with obvious weathered surfaces or impurities were discarded. Feldspar samples were crushed in a jaw crusher, ground in a disk mill, and then sieved to collect the 125–250 μm size fraction. Feldspar mineral sand was then rinsed and sonicated approximately 50 times in distilled deionized water until the supernatant was clear. In previous dissolution experiments, feldspar samples treated in this way displayed initial parabolic kinetics due to rapid dissolution of fine particles and strained sites on the mineral surfaces (e.g., Welch and Ullman 1993). Consequently, the feldspar sand was further washed in 0.1 m*M* HCl several times for several hours and then again in distilled deionized water to decrease this experimental artifact. This washing procedure was not expected to significantly alter feldspar mineral surface chemistry, because dissolution of the framework ions, Si and Al, is approximately stoichiometric at this pH (Welch and Ullman 1993). Surface area of the feldspar sand was measured using the BET method with krypton gas (Lowell and Shields 1984) and is approximately 0.16 m^2/g.

Bulk biotite samples were cut into pieces less than 10 mm in diameter and 5 mm thick using scissors and razor blades. Biotite samples were suspended in water and ground in a blender for several minutes. The slurry was then sieved to collect the 0.5 to 1 mm size fraction. Mineral samples were then washed and sonicated approximately 50 times in distilled water until the supernatant was clear. Biotite samples were air dried before dissolution experiments.

Experiments

Mineral dissolution experiments were run in batch reactors. For the dissolution and cryo-SEM experiments, minerals were dissolved in dilute $NaHCO_3$-HCl solutions (initial pH ≈ 6–7) with added nutrients for the bacteria.

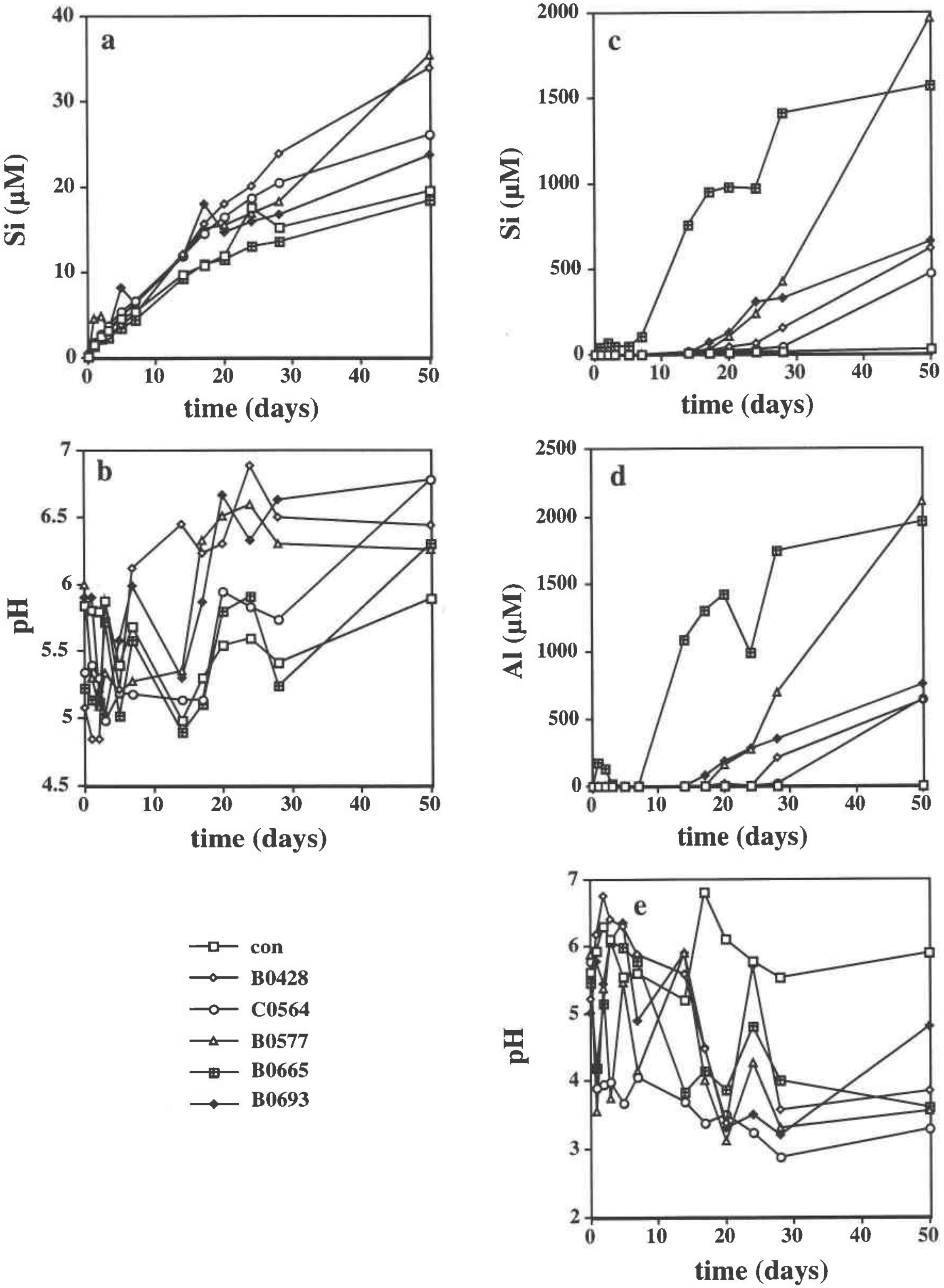
a
Si (µM)
0
10
20
30
40
time (days)
0
10
20
30
40
50
c
Si (µM)
0
500
1000
1500
2000
time (days)
b
pH
4.5
5
5.5
6
6.5
7
time (days)
d
Al (µM)
0
500
1000
1500
2000
2500
time (days)
e
pH
2
3
4
5
6
7
time (days)
con
B0428
C0564
B0577
B0665
B0693

One gram of feldspar or biotite sand was added to 100 mL of solution in an acid-washed polypropylene bottle. The experiments were not replicated, although in similar dissolution experiments with these minerals, results of replicate experiments were generally reproducible within 10% relative standard deviation (Vandevivere et al. 1994; Welch 1996). The experiments with bacteria had solution compositions that initially contained approximately 10^8 cells/mL of one of the five bacterial strains, 100 μM $NaNO_3$, and 10 μM Na_2HPO_4. For each solution that contained one of the bacterial strains, two experiments were performed. One experiment contained 1 mM glucose for metabolizing cells and the other did not contain glucose for non-metabolizing cells. Each of these two experiments was carried out against an abiotic control that had exactly the same solution composition including added nutrients (glucose, $NaNO_3$, and Na_2HPO_4), but lacked the bacteria. In the glucose treatment, glucose concentrations were monitored periodically (every few days) using a Stanbio glucose enzymatic test kit and glucose was replenished when concentrations were undetectable. Total glucose concentrations were in the range $\leq$0.1–2 mM. Five milliliter solution aliquots were removed from each bottle periodically and analyzed for pH and mineral ions. Solution pH was measured using an Orion pH meter calibrated with NBS buffers. Dissolved Si was measured using the molybdate blue method on a Technicon AutoAnalyser II. Standard addition experiments showed no apparent matrix effects with this method. For the feldspar dissolution experiments, total Al was measured using a Perkin Elmer graphite furnace atomic absorption spectrometer or by the catechol violet colorimetric method (Dougan and Wilson 1974). In the biotite dissolution experiments, total dissolved Fe was measured by the ferrozine method (Stookey 1970).

Epifluorescence microscopy

Mineral samples were removed from the reaction vessel every few days, stained with a 1.5 µg/mL solution of DAPI (4,6-diamidino-2-phenylindole), and examined with epifluoresence microscopy using a Leica DMR light microscope equipped with a 50X PL Fluotar objective lens.

Cryomicroscopy

Upon extensive microbial colonization of mineral surfaces (after several weeks), an aliquot of the mineral grains was removed for high-pressure cryofixation and cryo-SEM analysis. Specimens were placed between two gold planchets approximately 3 mm in diameter and cryofixed in a Balzers HPM 010 high-pressure freezer using liquid nitrogen within 10 ms at 2.1 kbar. Samples were partially freeze-dried and coated with 1.5 nm platinum using electron beam deposition in a Balzers MED 010 argon ion beam cryo-sputter coater. Samples were held at −95 °C in a cryostage and stereomicrographs recorded using a Hitachi S900 field-emission, low-voltage, high-resolution SEM operated at 1 kV.

Quantitative confocal microscopy

Solution parameters for the confocal measurements were similar to the dissolution and cryo-SEM experiments except initial glucose concentrations were 10 mM. Colonized biotite samples from microbial cultures were placed in a microscopy chamber (Chu et al. 1995) and perfused with 20 μM HEPES (N-[2-hydroxyethyl] piperazine-N′-[2-ethanesulfonic acid]) buffer at pH 7. Ratiometric pH measurements were made using 0.01 mM CL-NERF (cell impermeant pH sensitive dye designed for acidic conditions, Molecular Probes) and 0.5 mM Lucifer yellow (pH insensitive LY Lithium salt, Molecular Probes). The fluorescence yield of these dyes is not affected by changes in Eh (Ian Clements, Molecular Probes, personal communication). The fluorochromes were excited using an Ar laser (488 nm line at full power) and two images were collected simultaneously at 620–680 nm (for Lucifer Yellow) and 500–600 nm (for CL NERF) using a Zeiss LSM 410 confocal microscope equipped with a Zeiss C-Apo 40X objective lens. Ratio values were calibrated vs. pH using calibration curves of the same dye solution titrated to pH values from 2 to 6, imaged on the confocal microscope stage. Digital image slices collected in the XY plane were computer-manipulated to yield XZ images. Spatial resolution was better than 1 µm in all dimensions. All quantitative imaging procedures were similar to those described previously for use with biological specimens (Chu et al. 1995). Image analysis was performed using Metamorph (Universal Imaging).

RESULTS

Solution chemistry

Release of major structural elements, dissolved Si and Al for feldspar, and Si and Fe for biotite were used as an

←

FIGURE 1. Feldspar dissolution experiments in microbial cultures (B0428, C0564, B0577, B0665, B0693) and in an abiotic control. (**a**) Si release from feldspar over time in nonmetabolizing (no glucose) microbial cultures. (**b**) Bulk solution pH in nonmetabolizing (no glucose) microbial cultures and an abiotic control. (**c**) Si release from feldspar in glucose-metabolizing microbial cultures and an abiotic control. (**d**) Al release from feldspar in glucose-metabolizing microbial cultures and an abiotic control. (**e**) Bulk solution pH in glucose-metabolizing microbial cultures and an abiotic control. Dissolved Al is undetectable in the controls and in the nonmetabolizing microbial cultures. The sharp increase in Si and Al release from feldspars in the microbial cultures corresponds to the production of acids, extracellular polymers, and extensive microbial colonization of mineral surfaces.

overall indicator of mineral dissolution in these experiments (Figs. 1 and 2). Several previous experimental weathering studies have shown that release of these framework elements is most sensitive to changes in solution chemistry (Acker and Bricker 1992; Welch and Ullman 1993). In contrast, Na, Ca, and K, are preferentially leached from the mineral. There is often no systematic variation in cation leaching with changes in solution chemistry (Welch and Ullman 1993). In our dissolution experiments with nonmetabolizing bacteria (no glucose), dissolved Si release is at most a factor of two higher in microbial cultures compared to abiotic controls (Figs. 1a and 2a). Solution pH varied between approximately 5 and 7 (Figs. 1b and 2b), and dissolved Al and Fe were not detectable. The small increase in mineral dissolution in these experiments may reflect complexing of mineral ions by microbial cell surfaces. The increase also may be the result of lysis of microbial cells, which releases low molecular weight ligands to solution, thereby catalyzing mineral dissolution.

In contrast to the nonmetabolizing bacteria, the cultures with added glucose greatly increased Si, Al, and Fe release to solution by producing organic ligands and lowering solution pH (Figs. 1 and 2). Final dissolved Si concentrations were five to 100 times higher in the microbial cultures than in the abiotic controls by the end of the experiment. However this effect was not constant over time. With the exception of strain B0665, the bacteria had only a minimal effect on Si, Al, and Fe release from minerals compared to the controls in the first one to two weeks of the experiment. During this time, most of the bacteria were in suspension, the mineral surfaces were only sparsely colonized, and the bulk solution pH was generally >5 (Figs. 1e and 2e). After this initial lag phase however, all bacteria produced copious amounts of acids (both organic and inorganic) and lowered bulk solution pH to between 3 and 5. Although organic acids were not measured in these experiments, in previous experiments these strains of bacteria produced several organic acids including gluconate, lactate, acetate, and unidentified α-keto acids (Vandevivere et al. 1994). They also produced extracellular polymers that coated minerals and "glued" mineral grains together in the reaction vessel (Fig. 3). The production of acid, organic ligands, and extensive microbial colonization of the mineral surfaces greatly accelerated the release of mineral elements to solution.

Cryomicroscopy

Cryo-SEM images reproduce the three-dimensional hydrated structures formed by bacteria attached to mineral surfaces without the sample preparation artifacts associated with other SEM techniques. Microbial polysaccharides are commonly observed as either patchy films, stringy structures, or web-like structures. Figure 4 shows cryo-SEM images of a stalked bacteria (C0564) attached to a feldspar surface removed from culture approximately three weeks after the experiment started. In the upper part of Figure 4a are several rounded intact microbial cells that were presumably alive when cryofixed. A clump of dead "deflated" cells and cellular debris appear in the lower part of the image. The feldspar surface is sparsely covered with small (<0.1 μm) particles whose nature and composition are unknown. These particles could be mineralogical, created during the sample preparation or secondary phases formed during the experiment. Alternatively the particles may be biological in origin, either microbial extracellular polymers or cell debris. The surface of the feldspar does not appear to be extensively altered or etched by the attached bacteria in this area.

Figure 4b shows a row of bacteria that are oriented approximately parallel to cleavage steps along a broken feldspar surface. Unlike the previous image, the microbial cells and feldspar surface are covered with a "ropy" or "web-like" extracellular polymer. Figure 4c is a higher magnification of the previous image, showing microbial mucopolysaccharides adsorbed to rounded cleavage steps on the feldspar surface. The feldspar surfaces appear to be rough, presumably etched by microbial metabolites produced by adjacent microbial cells. The difference in the appearance between the more pristine feldspar surface in Figure 4a compared to 4b and 4c may be the result of heterogeneity on the feldspar surface, causing differential reaction rates. Alternatively, the differences could result from varying microbial residence times. The bacteria depicted in Figures 4b and 4c with their associated polymers likely colonized the mineral surfaces earlier in the experiment than those in Figure 4a.

Figure 5 shows feldspar surfaces reacted in a culture of B0693 for approximately three weeks. Release of framework elements (Si + Al) from feldspar was approximately an order of magnitude greater with this strain of bacteria compared to C0564 (Fig. 1). The total thickness of feldspar dissolved in this experiment is equivalent to

→

FIGURE 2. Biotite dissolution experiments in microbial cultures (B0428, C0564, B0577, B0665, B0693) and in an abiotic control. (**a**) Si release from biotite over time in nonmetabolizing (no glucose) microbial cultures. (**b**) Bulk solution pH in nonmetabolizing (no glucose) microbial cultures and an abiotic control. (**c**) Si release from biotite in glucose-metabolizing microbial cultures and an abiotic control. (**d**) Fe release from biotite in glucose-metabolizing microbial cultures and an abiotic control. (**e**) Bulk solution pH in glucose-metabolizing microbial cultures and an abiotic control. Dissolved Fe is undetectable in the controls and in the nonmetabolizing microbial cultures. The sharp increase in Si and Fe release from biotite in the microbial cultures corresponds to the production of acids, extracellular polymers, and extensive microbial colonization of mineral surfaces.

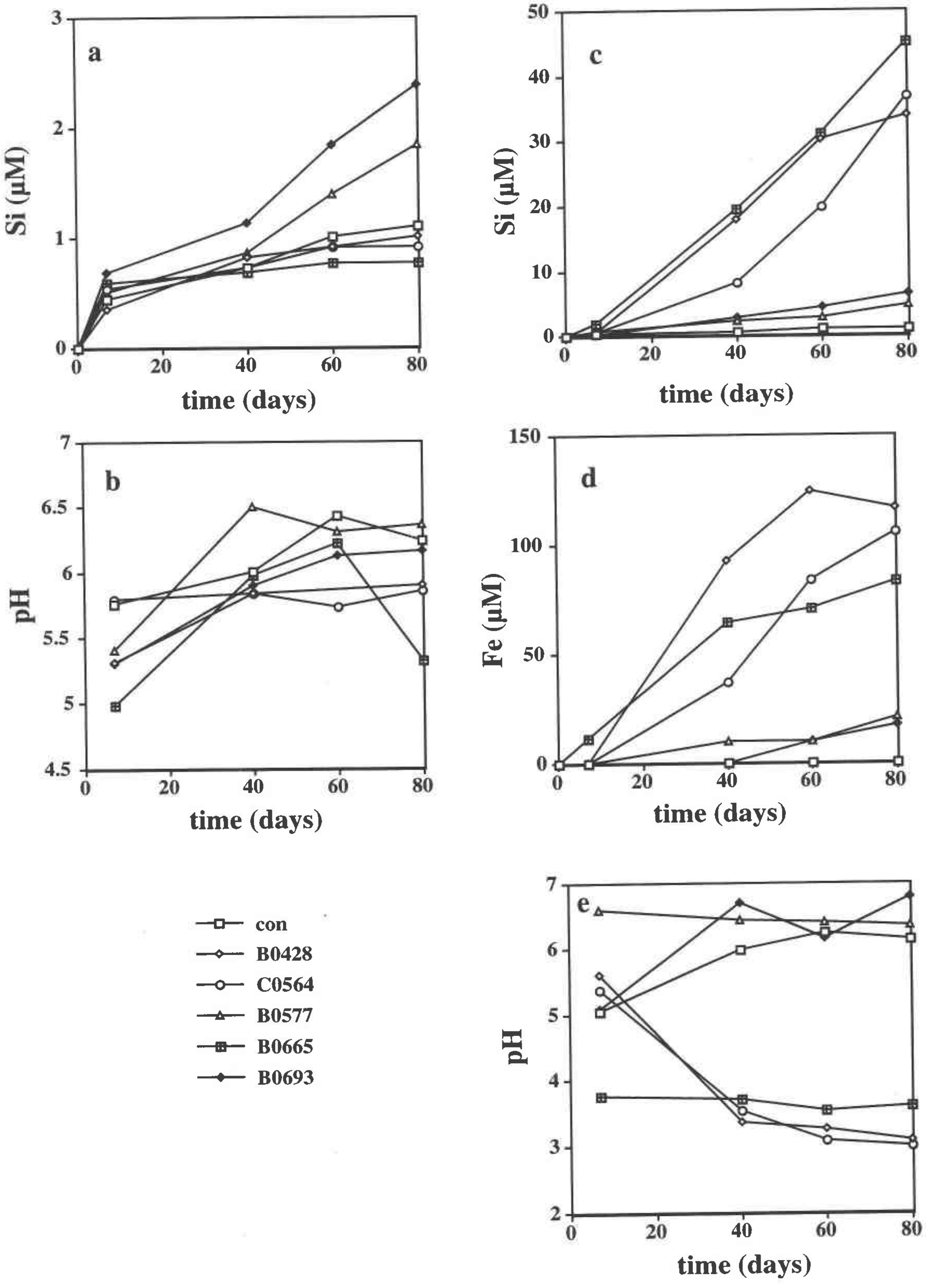
a
Si (µM)
0
1
2
3
time (days)
0
20
40
60
80
b
pH
4.5
5
5.5
6
6.5
7
time (days)
c
Si (µM)
0
10
20
30
40
50
time (days)
d
Fe (µM)
0
50
100
150
time (days)
e
pH
2
3
4
5
6
7
time (days)
con
B0428
C0564
B0577
B0665
B0693

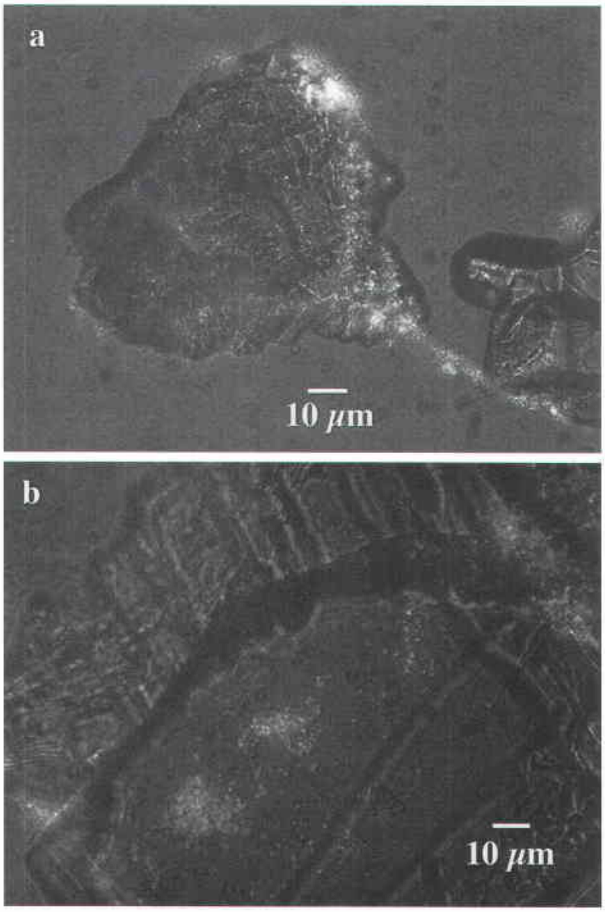

FIGURE 3. Epifluorescence microscopy images of bacteria on feldspar surfaces. Bacteria are stained with DAPI and appear as bright spots (≈1 μm) on feldspar surfaces. (**a**) Microbial production of extracellular polysaccharides binds feldspar grains together. (**b**) The distribution of bacteria on feldspar surfaces is heterogeneous; cells are found in small colonies or as isolated individuals on the surface.

~150 angstroms, or ~10 unit cells over the entire feldspar surface. This strain of bacteria is known for its ability to produce copious amounts of extracellular polysaccharides (Welch and Vandevivere 1994) as well as excrete low molecular weight ligands (Vandevivere et al. 1994). Figure 5a shows a feldspar grain coated with a thick microbial biofilm. In the upper part of the picture, the feldspar mineral is covered with a biofilm, and bacteria are visible as approximately 1 μm size circles or ovals at the surface. In the middle of the image one can see a several micrometers thick cross section of the biofilm that was exposed as the sample spontaneously cryofractured prior to etching. In the lower part of the picture, the biofilm has been removed from the feldspar surface, revealing a highly etched grain. The exposed mineral surface is very rough (contrast with Fig. 4a) and marked by etch pits from several tens of nanometers to several micrometers in size. Figure 5b is a red-green stereomicrograph, showing the delicate web-like structure of the biofilm. This

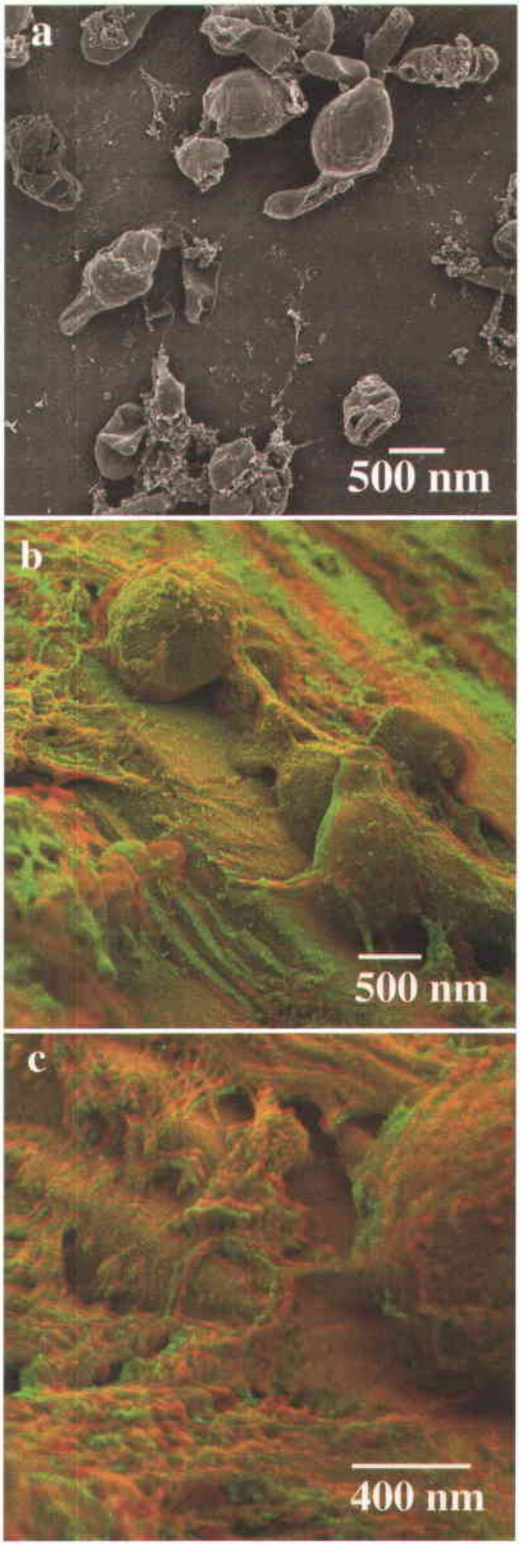

FIGURE 4. Cryo-SEM images of bacteria, C0564 on feldspar surfaces. (**a**) Bacterial cells and cell debris on a feldspar surface. (**b**) Red-green stereo image of cells oriented parallel to feldspar cleavage steps. (**c**) Higher magnification stereo image of bacterium attached via extracellular polymers to a feldspar surface.

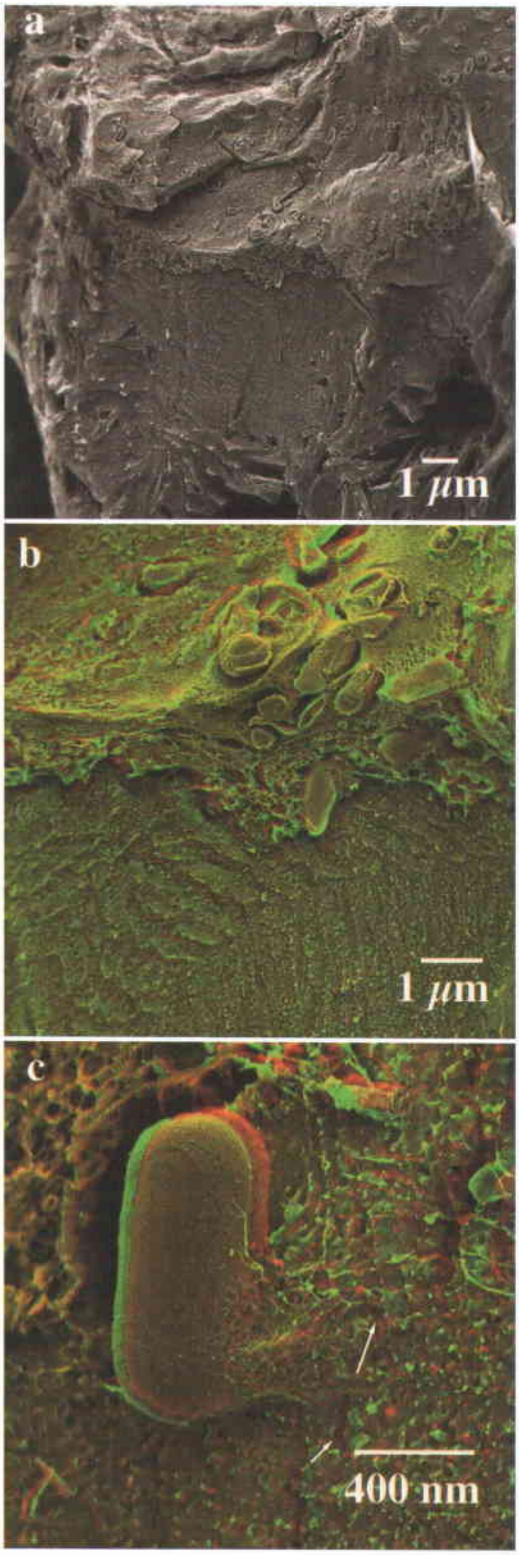

Figure 5. Cryo-SEM images of a microbial biofilm formed by B0693 on feldspar surfaces. (**a**) Low magnification image of biofilm covering the upper half of a mineral grain. Bacteria are visible as <1 μm sized circles or ovals. (**b**) Red-green stereopair of a cross section through the biofilm. (**c**) Red-green stereopair of bacteria attached to feldspar surface. Arrows denote two of the numerous etch pits and cracks formed on the mineral surface.

biofilm is heterogeneous and appears to consist of microbial cells within open pockets and densely packed mucopolysaccharide strands. The biofilm is an open structure, with ~5–10% of its volume consisting of pores >100 nm across and 20–50% consisting of pores 10–100 nm in size. Small etch pits and cracks are evident on the rough feldspar surface at this magnification. Open channels represent zones where nutrients can diffuse to microbial cells within the biofilm and solutes released from the feldspar surface can migrate to the bulk solution. Though the biofilm structure is fairly open, it forms a diffusion-limited zone, where conditions (pH, concentrations, redox) may differ from the bulk solution. Figure 5c shows a higher magnification image of one of the microbial cells in Figure 5a. The bacterium is attached to the mineral surface via a polysaccharide holdfast.

Figure 6 shows cryo-SEM images of biotite from a culture of the bacteria B0428. In Figure 6a, several stalked bacteria are attached to the biotite surface. In this experiment, however, the microbes have not yet produced significant quantities of extracellular polysaccharides. The attachment structure actually covers a much smaller mineral surface area than would a microbial cell resting on the surface. Bacteria often attach preferentially along cleavage planes or steps on a mineral surface. In Figure 6b, two bacteria are attached to the edge of a biotite grain within the 001 cleavage space. In Figure 6c, bacteria are attached along steps along a biotite (001) cleavage face. Bacteria also have several smaller mineral grains stuck tangentially to their surfaces.

Quantitative confocal microscopy

Figure 7 shows a series of six XZ sections (computer constructions from 1 μm thick optical XY slices) of an acid and polysaccharide producing bacterium (B0693) colonizing a biotite grain. The dark blue horizontal zones represent non-fluorescing biotite layers and the green strips the fluorescent dye solution filling interlayer spaces formed along open (001) cleavage planes or the "dye ocean" (bulk solution) surrounding the mineral. Figure 7a shows a cross section of an approximately 3 μm wide opening along a biotite (001) cleavage plane. The pH of the solution within the interlayer space is 3.5–4. Several bacteria are clearly visible in Figure 7b as approximately 1 μm dark ovals in the green interlayer space. The pH in this microenvironment ranged from approximately 3 to 4, although there was no observable pH gradient immediately surrounding the microbial cells. The pH in the void space on the right side of the diagram was lower than on the left, and this may result from a limited exchange between the pore and bulk solutions due to the presence of the microbial colony. Figure 7c, 7d, and 7e show bacteria within two parallel interlayer spaces, with low pH in these microenvironments. The wide green zone above the biotite grain in Figure 7f is the dye ocean or bulk solution, which is near neutral pH. The dark blue strip at the very top of Figure 7f is the non-fluorescing glass coverslip. Microbes colonizing the confined interlayer spaces

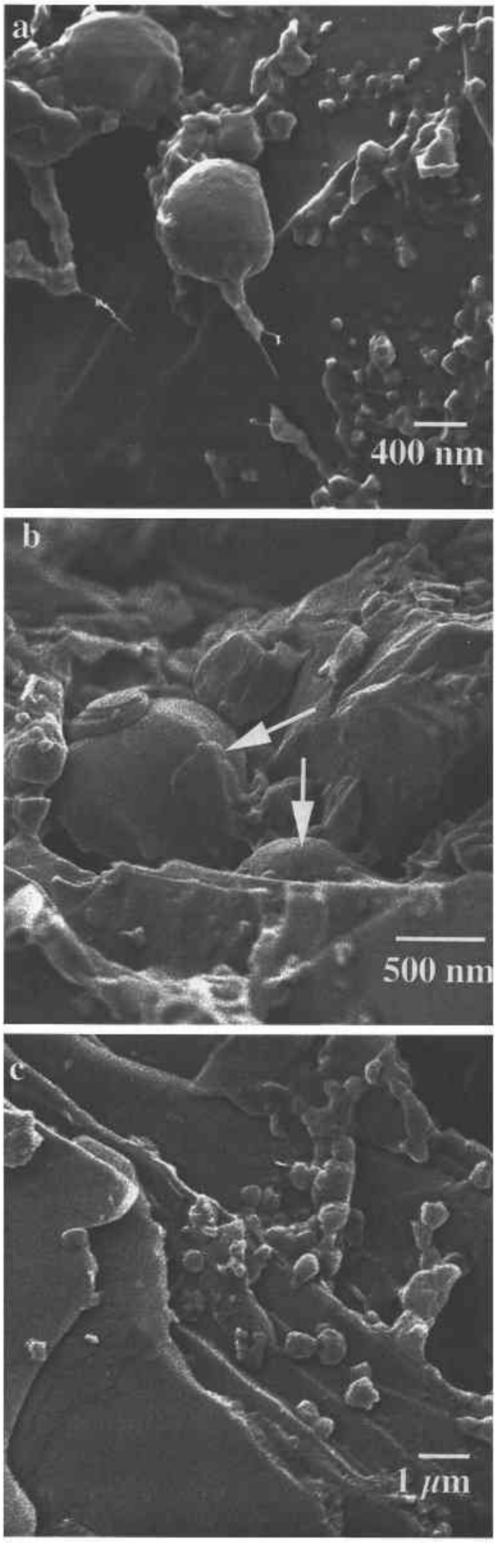

FIGURE 6. Cryo-SEM images of bacteria B0428 on biotite surfaces. (**a**) Stalked bacteria attached to biotite surfaces. (**b**) Two bacteria (arrows) colonizing biotite surface along (001) cleavage plane. (**c**) Many bacteria attached to (001) biotite surfaces.

were able to increase acidity by 3 to 4 orders of magnitude over the external bulk solution. Measurements were also made in uncolonized interlayer spaces as a control to ensure that no selective attenuation or filtering occurred during passage of the two fluorescent signals through biotite. No pH gradients occurred in uncolonized interlayers. Additionally, no decreased pH zone was detected in association with actively metabolizing bacterial microcolonies attached to the outer surfaces of biotite grains in these experiments.

DISCUSSION

There is considerable evidence from observations of naturally weathered minerals (Barker and Banfield 1996, 1998; Thorseth et al. 1992, 1995b), in situ field experiments (Bennett et al. 1996; Hiebert and Bennett 1992; Ullman et al. 1996), and in vitro experiments (Vandevivere et al. 1994; Thorseth et al. 1995a; Berthelin 1983) that microorganisms accelerate the degradation rates of rocks and minerals by both physical and chemical processes. Our dissolution experiments also demonstrate that microbial colonization of surfaces, production of inorganic and organic acids, and extracellular polymers greatly accelerates mineral weathering reactions and releases up to two orders of magnitude more material to solution than abiotic controls. The magnitude of these enhancement effects in natural environments and the mechanisms involved are still poorly understood. It is difficult to extrapolate in vitro results to natural conditions where nutrient concentrations, rates of microbial metabolism, microbial community structure, and mineral weathering rates vary widely. For example, while at first glance it might appear that high concentrations of free glucose are not readily available in the "bulk solution" in most natural environments, root exudates in rhizospheres often contain high concentrations of carbohydrates. Guckert et al. (1991) reported that *Beta vulgaris* released 1.1% of total root carbon as soluble exudates. Carbohydrates comprised 60% of this total and glucose accounted for 36% of total detected sugars.

The effect of microbially derived chemicals is amplified by increases in the amount of reactive surface area due to physical disruption by micro- and macroorganisms (Barker and Banfield 1996, 1998). Experiments conducted in this study show increases of up to four orders of magnitude in the activity of H^+ only within confined spaces of open biotite cleavages colonized by bacterial microcolonies. This result is consistent with in situ measurements of more macroscopic microenvironments via other techniques. For example, extremely low pH values, less than 3 to as low as 1, have been measured in a microbial biofilm forming on corroded metal in a marine environment using microelectrodes (Parasuraman 1995). pH gradients from approximately 8, the pH of the bulk seawater solution, to pH 1 occurred on the scale of several micrometers due to acid generated by metal redox reactions. We attribute the lack of pH gradients surrounding microcolonies on exterior biotite surfaces to diffusion

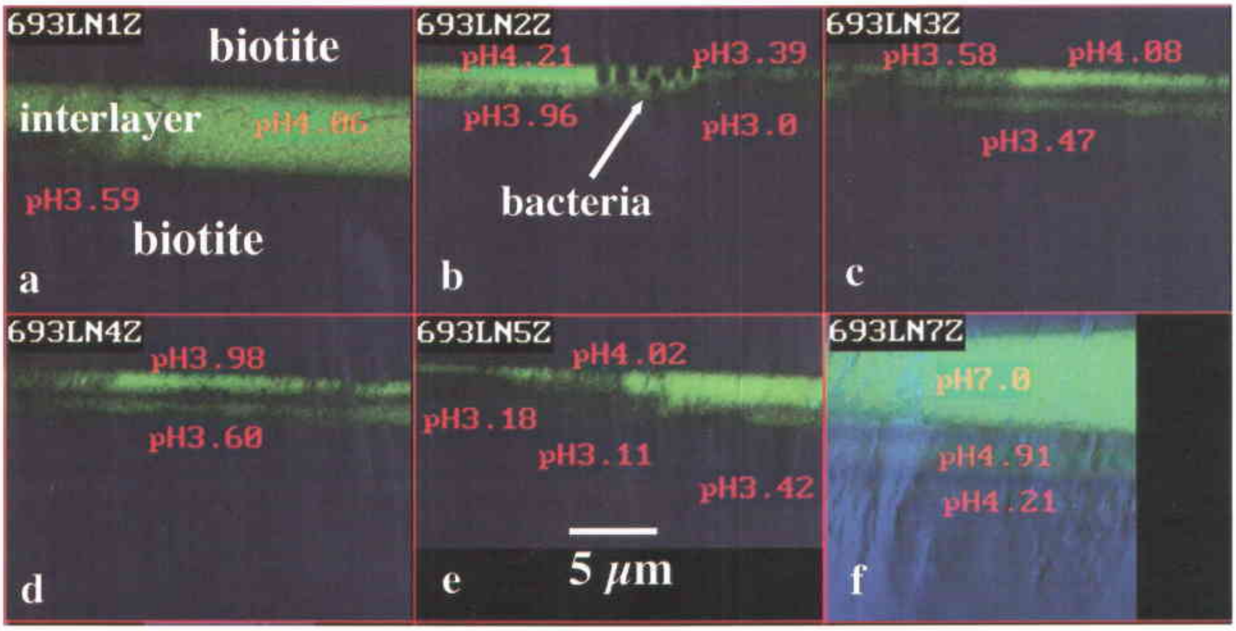

FIGURE 7. Quantitative ratiometric pH CSLM images of bacteria B0693, colonizing interlayer spaces within biotite.

of low molecular weight soluble ligands to bulk solution through a relatively thin biofilm. However, pH gradient have been measured surrounding microbial cells using confocal microscopy. Hassan et al. (1995a, 1995b) detected a decrease of approximately 1 pH unit in a microbial capsule surrounding lactic acid bacteria compared to the bulk solution. Small changes in pH have also been detected within millimeters of a root, from 7.5 to 6.5, with lower pH in the subapical zone (Ruiz and Arvieu 1990).

The pH dependence of aluminosilicate mineral weathering in acid solutions can be written as:

$$r = \mathrm{k}a^{n}_{\mathrm{H}^+}$$

where the exponent, n, is related to proton adsorption to the mineral surface (Blum and Lasaga 1988). For biotite dissolution, n is approximately 0.34 (Acker and Bricker 1992), so a decrease in solution pH from 7 to 3 corresponds to an approximately 20 times increase in dissolution rate. The experimentally determined pH dependence of feldspar dissolution in abiotic acidic solutions ranges from approximately $n = 0.3$ for albite to $n = 1$ for bytownite (Welch and Ullman 1996; Brady and Walther 1989), corresponding to a 10–1000 fold increase in mineral dissolution rates as pH decreases from 6 to 3. In our experiments, the extent of microbial coverage of the mineral surface and generation of low pH microenvironments are unknown, but if we make a conservative estimate of 10% microbial coverage forming a pH 3 zone, then approximately 50% to over 99% of the mineral dissolution could be attributed to microbial acid production.

Not only does the rate of the aluminosilicate dissolution reaction increase with acidity, the reaction mechanism and dissolution stoichiometry change as well. Feldspars dissolve incongruently at neutral pH, nonstructural ions (Na, Ca, K) are preferentially leached from the surface, and Si is preferentially released with respect to Al. As acidity increases, however, Al/Si release increases (Welch and Ullman 1993) leaving a residual material enriched in Si but depleted in other cations (Casey et al. 1989a, 1989b). In some abiotic dissolution experiments at neutral pH, biotite weathering is predominantly incongruent. The mechanism involves loss of interlayer cations, frequently charge balanced by oxidation of Fe^{2+} to Fe^{3+}, and inheritance of the 2:1 layer (Banfield and Eggleton 1988; Kogure and Murakami 1996). Acidification can change this process, resulting in a switch to congruent dissolution with an associated dramatic increase in Fe release to solution and an overall acceleration of degradation of the aluminosilicate structure (Acker and Bricker 1992). Mg and K release increase with acidity but to a lesser extent. In our experiments, we observed a dramatic increase in both Si and Fe release due to microbial production of acids.

Our SEM images show that mineral surfaces are coated with a thick complex microbial biofilm that covers a much larger surface area than the bacteria alone. Mineral surfaces underneath these microbial extracellular polymers were often extensively etched. Model rhizosphere studies in particular have demonstrated a strong correlation between proximity of microbial cells to mineral surfaces with increased K release from biotite. Berthelin and Belgy (1979) reported the complete removal of K and Ti from biotite in a granitic sand by a community of bacteria and fungi after a 22 week perfusion experiment, resulting in brittle, white micaceous particles.

Confocal XZ sections shown in this paper demonstrate extensive bacterial colonization of open (001) cleavages. Berthelin and Leyval (1982) found that symbiotic microorganisms in the rhizosphere increased the availability of K from biotite to *Zea mays,* and further noted that addition of nonsymbiotic microorganisms promoted much more biotite weathering and K uptake, an effect they attributed to "better soil exploration," which is essentially the ability of microorganisms to gain increased access to mineral surfaces. Frankel (1977) attributed weathering of biotite in estuarine sands to interlayer penetration by microorganisms. More recently Leyval and Berthelin (1991) confirmed these results by investigating the ability of rhizosphere microorganisms of pine to extract K from phlogopite. A far more interesting result was their report of a spatial correlation between rhizosphere microorganisms and areas of highest K depletion. Fritz et al. (1994) documented a similar K gradient in soil solutions from pine rhizosphere communities. This may be explained by the fact that microbes are a sink for K, and biotite weathering rates are strongly dependent on the concentration of K in solution.

Experimental weathering studies have demonstrated that microbial extracellular polymers can react chemically with mineral surfaces and mineral ions, increasing dissolution by up to several orders of magnitude (Welch et al., in preparation). Of particular interest are the results of Malinovskaya et al. (1990), who determined that mixtures of polymers and low molecular weight ligands had a synergistic effect on mineral weathering. This effect also may partly explain our dissolution data, because several species of the bacteria produced exopolymers and low molecular weight ligands.

Aluminosilicate weathering in natural environments occurs in an extremely complicated and dynamic system. Whereas some combination of hydration and oxidation reactions characterize the majority of low temperature mineral transformations, the presence of complex polymeric organic coatings on reacting mineral surfaces, fluctuating water potential and temperatures, and chemical microenvironments generated by a diverse community of actively metabolizing organisms greatly complicate weathering. In these experiments we have used novel techniques to characterize the interaction of naturally occurring soil bacteria with two common aluminosilicates. While advanced cryotechniques in electron microscopy have seen limited use in geomicrobiology, they clearly offer the best possibility for examining the true hydrated three-dimensional textures and structures of biofilm architecture. Similarly, the potential of quantitative confocal scanning laser microscopy has not been realized in studying mineral–microbe interactions. The ability to study pH microdomains, as well as examine gradients and concentrations of several important metal ions, in living systems, has the potential to revolutionize our understanding of elemental partitioning between minerals and biological systems. Complete integration of field observations, laboratory experiments, and various light and electron microscopies is necessary to explore these labyrinthine ecosystems.

ACKNOWLEDGMENTS

We thank Marshall Montrose for gracious use of his confocal laboratory. Colleen Lavin (high-pressure cryofixation) and Ya Chen (Hitachi S900), participated via NIH Biomedical Research Technology Grant 00570 to the Integrated Microscopy Resource, Madison, Wisconsin. Reviewers Patricia Dove and Philip Bennett greatly improved the manuscript. This research was supported by grant no. DEFG02-93ER14328 from the Office of Basic Energy Sciences of the U.S. Department of Energy.

REFERENCES CITED

Acker, J.G. and Bricker, O.P. (1992) The influence of pH on biotite dissolution and alteration kinetics at low temperature. Geochimica et Cosmochimica Acta, 56, 3073–3092.

Antweiler, R.C. and Drever, J.I. (1983) The weathering of a late Tertiary volcanic ash: importance of organic solutes. Geochimica et Cosmochimica Acta, 47, 623–629.

Banfield, J.F. and Eggleton, R.A. (1988) A transmission electron microscope study of biotite weathering. Clays and Clay Minerals, 36, 47–60.

Banfield, J.F. and Nealson, K.H (1997) Geomicrobiology: Interactions between microbes and minerals. Mineralogical Society of America Reviews in Mineralogy, 35, 448.

Barker, W.W. and Banfield, J.F. (1996) Biologically versus inorganically-mediated weathering reactions: Relationships between minerals and extracellular microbial polymers in lithobiontic communities. Chemical Geology, 132, 5–69.

———(1998) Zones of chemical and physical interaction at interfaces between microbial communities and minerals. A model. Geomicrobiology Journal, 15, 223–244.

Barker, W.W., Welch, S.A, and Banfield, J.F. (1997) Geomicrobiology of silicate mineral weathering. In Mineralogical Society of America Reviews in Mineralogy, 35, 391–428.

Bennett, P.C., Hiebert, F.K., and Choi, W.J. (1996) Microbial colonization and weathering of silicates in a petroleum-contaminated groundwater. Chemical Geology, 132, 45–53.

Berthelin, J. (1983) Microbial weathering processes. In W.E. Krumbein, Ed., Microbial Geochemistry, p. 223–262. Blackwell Scientific Publications, Oxford, U.K.

Berthelin, J. and Belgy, G. (1979) Microbial degradation of phyllosilicates during simulated podzolization. Geoderma, 21, 297–310.

Berthelin, J. and Leyval, C. (1982) Ability of symbiotic and non-symbiotic rhizospheric microflora of maize (*Zea mays*) to weather micas and to promote plant growth and plant nutrition. Plant and Soil, 68, 369–377.

Blum, A. and Lasaga, A.C. (1988) Role of surface speciation in the low temperature dissolution of minerals. Nature, 331, 431–433.

Brady, P.V. and Walther, J.V. (1989) Controls on silicate dissolution rates in neutral and basic pH solutions at 25°C. Geochimica et Cosmochimica Acta, 53, 2823–2830.

Casey, W.H., Westrich, H.R., Massis, T., Banfield, J.F., and Arnold, G.W. (1989a) The surface of labradorite feldspar after acid hydrolysis. Chemical Geology, 78, 205–218.

Casey, W.H., Westrich, H.R., Arnold, G.W., and Banfield, J.F. (1989b) The surface chemistry of dissolving labradorite feldspar. Geochimica et Cosmochimica. Acta, 53, 821–832.

Chenu, C. and Roberson, E.B. (1996) Diffusion of glucose in microbial extracellular polysaccharide as affected by water potential. Soil Biology and Biochemistry, 28, 877–884.

Christensen, B.E. and Characklis, W.G. (1990) Physical and chemical properties in biofilms. In W.G. Characklis and K.C. Marshall, Eds., Biofilms, p 93–130. Wiley, New York.

Chu, S., Brownell, W.E., and Montrose, M.H. (1995) Quantitative confocal imaging along the crypt-to-surface axis of colonic crypts. American Journal of Physiology, 269, c1557–c1564.

Chu, S. and Montrose, M.H. (1995) Extracellular pH regulation in microdomains of colonic crypts: Effects of short chain fatty acids. Proceedings of the National Academy of Sciences, 92, 3303–3307.

Defarge, C, Trichet, J., Jaunet, A.-M., Robert, M., Tribble, J., and Sansone, F.J. (1996) Texture of microbial sediments revealed by cryo-scanning electron microscopy. Journal of Sedimentary Research, 66, 935–947.

Dougan, W.K. and Wilson, A.L. (1974) The absorptiometric determination of aluminum in water. A comparison of some chromogenic reagents and the development of an improved method. Analyst, 99, 413–430.

Echlin, P. (1992) Low-Temperature Microscopy and Analysis, 539 p. Plenum Press, New York,

Ehrlich, H.L. (1996) Geomicrobiology, 717 p. Marcel Dekker, Inc., New York.

Fortin, D., Ferris, F.G., and Beveridge, T.J. (1997) Surface-mediated mineral development by bacteria. In Mineralogical Society of America Reviews in Mineralogy, 35, 161–180.

Frankel, L. (1977) Microorganism induced weathering of biotite and hornblende grains in estuarine sands. Journal of Sedimentary Petrology, 47, 849–854.

Fredrich, J.T., Menendez, B., and Wong, T.-F. (1995) Imaging the structure of geomaterials. Science, 268, 276–279.

Fritz, E., Knoche, D., and Meyer, D. (1994) A new approach for rhizosphere research by X-ray microanalysis of micro-liter soils solutions. Plant and Soil, 161, 219–223.

Guckert, A., Chavanon, M., Mench, M., Morel, J.L., and Villemin, G. (1991) Root exudation in *Beta vulgaris*: a comparison with *Zea mays*. In B.L. McMichael and H. Persson, Eds., Developments in Agricultural and Managed-Forest Ecology 24. Plant Roots and Their Environment, p. 449–455. Elsevier, New York.

Hassan, A.N., Frank, J.F., Farmer, M.A., Schmidt, K.A., and Shalabi, S.I (1995a) Observation of encapsulated lactic acid bacteria using confocal scanning laser microscopy. Journal of Dairy Science, 78, 2624–2628.

——— (1995b) Formation of yogurt microstructure and the three dimensional visualization as determined by confocal scanning laser microscopy. Journal of Dairy Science, 78, 2629–2636.

Hiebert, F.K. and Bennett, P.C. (1992) Microbial control of silicate weathering in organic-rich ground water. Science, 258, 278–281.

Huang, P.M. and Schnitzer, M. (1986) Interactions of Soil Microbes with Natural Organics and Microbes. Soil Science Society of America Special Publication no. 17, 606 p. Soil Science Society of America, Madison, Wisconsin.

Kogure, T. and Murakami, T. (1996) Direct identification of biotite/vermiculite layers in hydrobiotite using high-resolution TEM. Mineralogical Journal, 18, 131–137.

Lawrence, J.R., Korber, D.R., Hoyle, B.D., Costerton, J.W., and Caldwell, D.E. (1991) Optical sectioning of microbial biofilms. Journal of Bacteriology, 173, 6558–6567.

Lawrence, J.R., Wolfaardt, G.M., and Korber, D.R. (1994) Determination of diffusion coefficients in biofilms by confocal laser microscopy. Applied and Environmental Microbiology, 60, 1166–1173.

Leyval, C. and Berthelin, J. (1991) Weathering of a mica by roots and rhizospheric microorganisms of pine. Soil Science Society of America Journal, 55, 1009–1016.

Little, B.J., Wagner, P.A., and Lewandowski, Z. (1997) Spatial relationships between bacteria and mineral surfaces. In Mineralogical Society of America Reviews in Mineralogy, 35, 123–159.

Lowell, S. and Shields, J.E. (1984) Powder Surface Area and Porosity, 234 p. Chapman and Hall, New York.

Malinovskaya, I.M., Kosenko, L.V., Votselko, S.K., and Podgorskii, V.S. (1990) Role of *Bacillus mucilagosus* polysaccharide in degradation of silicate minerals. Mikrobiologiya, 59, 49–55.

Ophir, T. and Gutnick, D.L. (1994) A role for exopolysaccharides in the protection of microorganisms from desiccation. Applied and Environmental Microbiology, 60, 740–745.

Parasuraman, C.S. (1995) Mechanism of potential ennoblement on passive metals due to biofilms in seawater. Doctoral dissertation, University of Delaware.

Pawley, J.B. (1995) Handbook of Biological Confocal Microscopy, 2nd ed., Plenum Press, New York. 632 p.

Petford, N. and Miller, J.A. (1992) Three-dimensional imaging of fission tracks using confocal scanning laser microscopy. American Mineralogist, 77, 52–533.

Rautureau, M., Cooke, R.U., and Boyde, A. (1993) The application of confocal microscopy to the study of stone weathering. Earth Surface Processes and Landforms, 18, 769–775.

Roos, W. (1992) Confocal pH topography in plant cells—Acidic layers in the periferal cytoplasm and the apoplast. Botanica Acta, 105, 253–259.

Ruiz, L. and Arvieu, J.C. (1990) Measurement of pH gradients in the rhizosphere. Symbiosis, 9, 71–75.

Steinbrecht, R.A. and Zierold, K. (1987) Cryotechniques in Biological Electron Microscopy, 297 p., Springer-Verlag, New York.

Stone, A.T. (1997) Reactions of extracellular organic ligands with dissolved metal ions and mineral surfaces. In Mineralogical Society of America Reviews in Mineralogy, 35, 309–344.

Stoodley, P., de Beer, D., and Lewandowski, Z. (1994) Liquid flow in biofilm systems. Applied and Environmental Microbiology, 60, 2711–2716.

Stookey, L.L. (1970) Ferrozine—a new spectrophotometric reagent for iron. Analytical Chemistry, 42, 779–781.

Sutherland, I.W. (1972) Bacterial exopolysaccharides, Advances in Microbial Physiology, 6, 142–213.

Thorseth, I.H., Furnes, H., and Heldal, M. (1992) The importance of microbial activity in the alteration of natural basaltic glass. Geochimica et Cosmochimica Acta, 56, 845–850.

Thorseth, I.H., Furnes, H., and Tumyr, O. (1995a) Textural and chemical effects of bacterial activity on basaltic glass: an experimental approach. Chemical Geology, 119, 139–160.

Thorseth, I.H., Torsvik, T., Furnes, H., and Muehlenbachs, K. (1995b) Microbes play an important role in the alteration of oceanic crust. Chemical Geology, 126, 137–146.

Ullman, W.J., Kirchman, D.L., Welch, S.A., and Vandevivere, P. (1996) Laboratory evidence for the microbially mediated silicate mineral dissolution in nature. Chemical Geology, 132, 11–17.

Vandevivere, P., Welch, S.A., Ullman, W.J., and Kirchman, D.L. (1994) Enhanced dissolution of silicate minerals by bacteria at near-neutral pH. Microbial Ecology, 27, 241–251.

Welch, S.A. (1996) Effect of bacteria and microbial metabolites on bytownite feldspar dissolution at Earth's surface temperature. Ph.D. dissertation, University of Delaware.

Welch, S.A. and Ullman, W.J. (1993) The effect of organic acids on plagioclase dissolution rates and stoichiometry. Geochimica et Cosmochimica Acta, 57, 2725–2736.

Welch, S.A. and Vandevivere, P. (1994) Effect of microbial and other naturally occurring polymers on mineral dissolution. Geomicrobiology Journal, 12, 227–238.

Welch, S.A. and Ullman, W.J. (1996) Feldspar dissolution in acidic and organic solutions: Compositional and pH dependence of dissolution rate. Geochimica et Cosmochimica Acta, 60, 2939–2948.

MANUSCRIPT RECEIVED FEBRUARY 23, 1998
MANUSCRIPT ACCEPTED AUGUST 5, 1998
PAPER HANDLED BY KATHRYN L. NAGY